PR2 Development on Neutron Imaging Application

Y. Saito

Research Reactor Institute, Kyoto University

1. Objectives and Allotted Research Subjects

Neutron imaging provides valuable information which cannot be obtained from an optical or X-ray imaging. The purpose of this project is to develop the imaging method itself and also the experimental environment for expanding the application area of the neutron imaging. The allotted research subjects are as follows:

ARS-1 Measurements of Multiphase Dynamics by Neutron Radiography (Y. Saito *et al.*)
ARS-2 Visualization and Measurement of Flow Behavior in Industrial Equipment (N. Takenaka *et al.*)
ARS-3 Visualization and Measurement of Adsorption/Desorption Process of Ethanol in Activated Carbon Adsorber for Adsorption Heat Pump (N. Asano *et al.*)
ARS-4 Neutron Radiography on Tubular Flow Reactor for Supercritical Hydrothermal Synthesis of Nanoparticles (T. Tsukada *et al.*)
ARS-5 Characteristics of the Void Fraction under Transient Condition (H. Umekawa *et al.*)
ARS-6 Estimation of the Frosting and Defrosting Phenomena by Using Netron Radiography (R. Matsumoto *et al.*)
ARS-7 Neutron imaging and optics development using simulation of VCAD Systems (Y. Yamagata *et al.*)
ARS-8 Water and Salt Distribution in a Rice Hull Medium under Sodium Chloride Solution Culture (U. Matsushima *et al.*)
ARS-9 Measurement of Water Content in Hardened Cement Paste by Neutron Imaging (T. Numao *et al.*)
ARS-10 Hydrazine Thickness Measurement by Neutron Radiography at a Catalyst Bed during Operation (H. Kagawa *et al.*)
ARS-11 In-situ Neutron Radiography Investigation on the Hydraulic Behavior of High Strength Cement Paste under High Temperature (M. Kanematsu *et al.*)
ARS-12 Evaluation of coolant distribution in a flat heat-pipe type heat spreader (K. Mizuta *et al.*)
ARS-13 Visualization of Organic Materials for Development of Industrial Applications (A. Uritani *et al.*)
ARS-14 Visualization of Coolant Flow in a Micro-Structured Wick (Y. Tsuji *et al.*)

2. Main results and the contents of this report

Due to the termination of KUR, no neutron imaging has been performed for fiscal 2015. However, some results have been obtained by analyzing existing experimental results or by performing X-ray imaging.

ARS-2 applied X-ray imaging to two-phase flow across horizontal tube bundles of in-line and staggered. X-ray radiography was employed for the measurement of void fraction distributions. The transmitted X-ray was converted to visible rays using an image intensifier, and the 10-bit gray-scale radiographs were taken using a high-speed camera (MotionPro Y-4 Lite, IDT Inc.) with an array of 1024 × 1024 pixels and with a pixel size of 170 μm. The flame rate was set at 30 fps and 450 radiographs which correspond to 15 sec were taken in each condition. The X-ray was generated at 80 kV and 5 mA.
heat transfer study on an adsorption refrigerator. In this ARS, visualization of adsorption amount distributions of ethanol in an activated carbon powder bed. Experimental results show that transient behaviors of adsorption amount distribution could be clearly observed by neutron radiography.

ARS-3 visualized transient change of adsorbed refrigerant amount during an adsorption process by using neutron imaging. From the measurement results effect of the metallic fins was investigated for improvement of heat diffusion in adsorption process.

In ARS-4, flow behavior of heavy oils in a packed-bed reactor was investigated by using B-4 neutron imaging facility. In this work, it was revealed that the visualization of flow behaviors of heavy oils in the packed-bed reactor at high temperature and high pressure is feasible by neutron radiography.

ARS-5 conducted frosting and defrosting experiments by using neutron/X-ray imaging. On the cooled surface of a heat exchanger, the frost grows with a spatial distribution that is determined by the temperature and humidity profiles of the air and the flow pattern in the heat exchanger. This means that the mass transfer coefficient for frost formation has both temporal and spatial distribution. However, in conventional methods of measuring the frost accumulation rate, the frost is scraped from the surface, or the frost accumulation is estimated from the difference between the absolute humidity before and after the heat exchanger. In the present study, the frost formation and defrosting process was estimated by the two ways by neutron and X-ray radiographies at KUR B-4 radiation port.

PR2-1 Void Fraction Distritbution around a Tube in Two-phase Flows Across Horizontal Tube Bundles

H. Murakawa, M. Baba, T. Miyazaki, K. Sugimoto,
H. Asano, N. Takenaka, D. Ito[1] and Y. Saito[1]

Department of Mechanical Engineering, Kobe University
[1]Research Reactor Institute, Kyoto University

INTRODUCTION: Heat exchangers such like shell and tube type are commonly used in process industry, chemical industry, and geothermal power plant. The void fraction in the flow channel are important parameters for predicting the flow characteristics, fluid oscillation and heat transfer. To clarify the two-phase flow structures, many experimental studies have been carried out in a rectangular channel with the tube bundle [1-4]. However, many of these investigation evaluate local void fraction at several measurement positions in the tube bundles, and the two-dimensional void fraction distributions in the bundles has not been sufficiently carried out.
In this study, two-dimensional void fractions were measured by using X-ray radiography in two-phase flow across horizontal tube bundles of in-line and staggered. Difference of void fraction distribution in each flow regime and bundle arraignment were compared.

EXPERIMENTS: The test section was vertical duct with a cross-section of 90 × 90 mm^2. Air was injected into the test section through two porous tubes located at the bottom of the test section. Two different tube bundles were employed for the measurements. One was an in-line tube bundle with 8 rows of three full tubes and two half tubes. And the other was a staggered tube bundle with 8 rows. The tube in both bundles were 90 mm long and the outer diameter, d, was 15 mm. The tubes pitch, p, was 22.5 mm and the pitch-to-diameter ratio, p/d, was 1.5. The experiments were performed at 20–25 ºC.
X-ray radiography was employed for the measurement of void fraction distributions. The transmitted X-ray was converted to visible rays using an image intensifier, and the 10-bit gray-scale radiographs were taken using a high-speed camera (MotionPro Y-4 Lite, IDT Inc.) with an array of 1024 × 1024 pixels and with a pixel size of 170 μm. The flame rate was set at 30 fps and 450 radiographs which correspond to 15 sec were taken in each condition. The X-ray was generated at 80 kV and 5 mA.

RESULTS: Results of two-dimensional void fraction distributions are shown in Fig. 1. The mass flux, G, is 200 kg/m^{2}s, and the superficial gas velocity, J_G, is 0.36 and 0.86 m/s. The measurement area is around center tube at 4th row from the inlet of the bundles.
For in-line tube bundle, many bubbles pass travel along the vertical tube gaps, and the void fraction became higher than that at the other region in bubbly flow. Some bubbles passing through the bottom of tubes. As a result, void fraction around the upstream of each tube becomes higher than that around downstream of the tubes. In intermittent flow regime, large bubble intermittently pass through the tubes. As a result, void fraction around the maximum gap and vertical minimum gap increased. The maximum void fraction around maximum and vertical minimum gaps were almost the same. However, void fraction around the horizontal minimum gap is slightly lower than that around maximum and vertical minimum gaps.
For staggered tube bundle, the void fraction around upstream of tubes is slightly high in comparison with the horizontal tube side. Tendency of the void fraction distribution is almost the same with that in in-line tube bundle, however, the void fraction around the bottom of tubes are slightly higher than that in the other region. At intermittent flow, void fraction around bottom of tubes became much higher than the other region. Therefore, it can be confirmed that large bubbles tend to be stagnant around the bottom of tubes. As a result, void fraction has large distribution in comparison with that in in-line tube bundle. Furthermore, the maximum void fraction in staggered tube bundle was higher than that in in-line tube bundle.

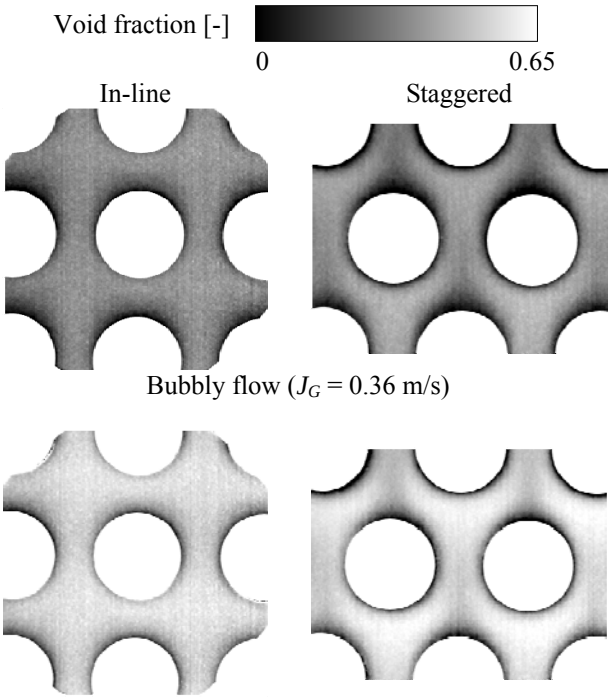

Fig. 1. Two-dimensional void-fraction distributions in in-line and staggered tube bundles.

REFERENCES:

[1] R. Dowlati *et al.*, AIChE Journal, **36** (1990) 765-772.
[2] R. Dowlati *et al.*, Tras. ASME, **114** (1992) 450-456. 1992.
[3] D.A. McNeil *et al.*, Int. J. Multiphase Flow, **45** (2012) 53-69.
[4] G.R. Noghrehkarm *et al.*, Int. J. Multiphase Flow, **25** (1999) 857-874.

PR2-2 Quantitative Measurement of Adsorbed Ethanol Amount in Activated Carbon Adsorber for Adsorption Heat Pump

H. Asano, K. Murata, N. Takenaka, H. Murakawa, K. Sugimoto, Y. Saito[1] and D. Ito[1]

Department of Mechanical Engineering, Kobe University
[1]Research Reactor Institute, Kyoto University

INTRODUCTION: Adsorption refrigerator is one of the efficient tools for waste heat utilization at low temperature. In the refrigerating cycle, adsorption and desorption processes are alternately repeated in batch operation. Since heat removal of latent heat of adsorbed refrigerant is necessary during the adsorption process, improvement of heat diffusion in adsorption layer. Although metallic fins are usually used for the enhancement in the heat diffusion, the amount of inserted fins should be minimized from the standpoint of the downhold of the heat capacity. It is important for the improvement of adsorber to clarify the distribution of adsorbed refrigerant amount in an adsorbent bed during transient conditions of adsorption/desorption. Neutron radiography was applied to visualize the adsorption amount distribution of ethanol in an activated carbon particle bed, and the effect of aluminum fins were evaluated from the measured results.

EXPERIMENTS: Activated carbon and ethanol was used as the adsorbent and refrigerant, respectively. The activated carbon MAXSORB® III produced by Kansai Coke and Chemical Co., Ltd. was used as the adsorbent. Activated carbon was packed in an aluminum frame shown in Figure 1. The container was connected to an ethanol reservoir. The vapor pressure in the container could be maintained by the temperature of the reservoir. The front and back wall was made of thin stainless steel plates to avoid heat diffusion through the walls. The adsorber could be cooled in adsorption process or heated in desorption process by water through a channel in the bottom wall. Two aluminum fins with the thickness of 1 mm were inserted in the adsorbent bed to enhance the heat diffusion. The mass attenuation coefficient of ethanol against thermal neutron was measured as 3.86 g/cm2 in our preliminary experiment.

RESULTS: Transient change of adsorbed refrigerant amount during an adsorption process was measured quantitatively by the umbra method using a checked-type neutron absorber. Figure 2 (a) shows a visualized image with the neutron absorber grid. The inside wall including the fins are indicated by white lines. The measured adsorbed amounts in the center section and temperature in the adsorption bed are shown in Fig. 2 (b) and (c), respectively. At the initial condition, the adsorbent was dry and vacuated. Then, by opening a valve between the ethanol reservoir and the test section, vapor ethanol was supplied to the test section. The horizontal axis of Fig. 2 (a) and (b) shows the elapsed time from the opening of the valve. Just after the start, the adsorbent temperature rapidly increased, and reached around 70 °C due to the strong adsorption. Then, adsorbed refrigerant amount gradually increased with a gradual decrease in the adsorbent temperature due to heat diffusion. The difference in the temperature of the adsorbent between T_{ad2} and T_{ad3} was little. The adsorption amounts in the area of 5, 7, and 8 near the heat transfer surfaces were larger than the amounts in the area of 6 during the transient condition. The fact means that the phenomenon is dominated by heat conduction in the adsorbent bed.

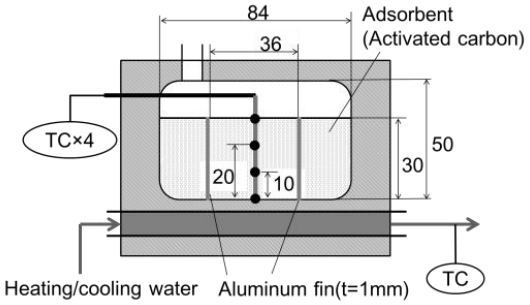

Fig. 1 Configuration of the test section.

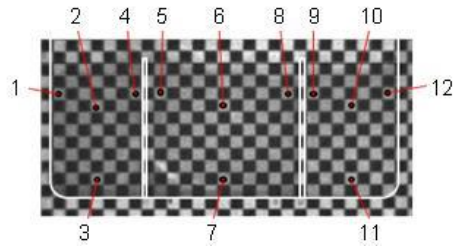

(a) Visualized image with neutron absorber grid

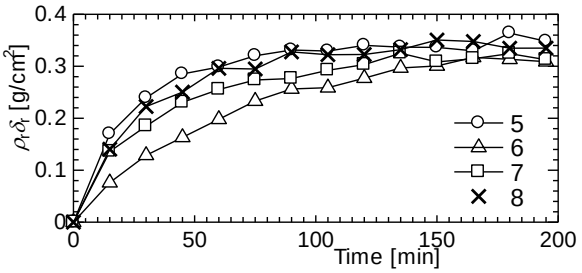

(b) Adsorbed refrigerant amount

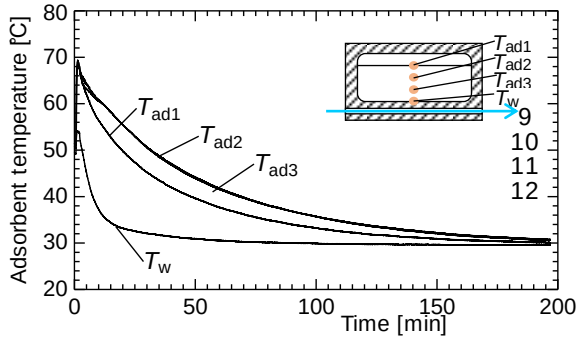

(c) Temperature in adsorption layer

Fig. 2 Transient change during adsorption process.

PR2-3 Neutron Radiography on Flow Behavior of Heavy Oils in Packed-Bed Reactor

T. Tsukada, K. Sugioka, M. Kubo, Y. Mukawa, S. Takami [1], T. Adschiri[2], K. Sugimoto[3], N. Takenaka[3], Y. Saito[4] and Y. Kawabata[4]

Dept. of Chemical Engineering, Tohoku University
[1]IMRAM, Tohoku University
[2]WPI-AIMR, Tohoku University
[3]Dept. of Mechanical Engineering, Kobe University
[4]RRI, Kyoto University

INTRODUCTION: With the increase of the demand for petrochemical feedstock and middle distillate, it is desired to utilize heavy crude oils and residues as new resources. However, as heavy oils have high viscosity and poor quality, the upgrading and refining processes of heavy oils are indispensable. For instance, a trickle-bed reactor is commonly used as the residue hydrodesulfurization unit of heavy oils, and thus, it is important to understand the flow behavior of heavy oils through a packed bed of catalyst pellets at high temperature and high pressure for design and optimization of the process. However, because of the reactor which is made of metal and the high-temperature and high-pressure processing, it is impossible to visualize directly the flow behavior inside the reactor. Therefore, we are going to use neutron radiography to visualize the flow behavior of heavy oils in a trickle-bed reactor. In this work, as a first step of such visualization, the flow behavior of bitumen through a packed bed were observed at atmospheric pressure using neutron radiography.

EXPERIMENTS: Fig.1 shows the schematic diagram of a packed-bed reactor, which was made of a SUS316 tube with outer diameter of 1/2 inch and contained alumina particles with 1 or 3 mm diameter. Heavy oil was fed to the reactor through SUS316 1/16 inch tube by using a high-pressure pump. The fourth of five fractions fractionated by vacuum distillation of bitumen was used as a sample. Here, the viscosity of the sample was adjusted by varying the temperature between 40 and 80℃.

Neutron radiography of the packed-bed reactor, i.e., the flow behavior of the sample through the packed bed, was carried out, where the neutron radiographs were taken by an image intensifier and a high speed camera. A thermal neutron beam emitted from the B4 port in KUR was used. The imaging method of neutron radiography and subsequent analysis of the images were almost similar to those in our previous work [1].

RESULTS: Figs. 2 (a) to (c) show the neutron radiographs of flow behaviors of packed-bed reactor, where (a) the temperature T = 69.8℃, the flow rate Q = 0.6 mL/min, and the diameter of particles D = 1 mm, (b) T = 73.0℃, Q = 0.6 mL/min, D = 3 mm, and (c) T = 44.2℃, Q = 0.6 mL/min and D = 3 mm. In the images, the dark part corresponds to the sample flowing downward through the packed bed. From the figures, it is found that the temperature in the reactor, i.e., the viscosity of the sample, and the diameter of packed materials affect the flow behaviors. The sample spreads to the radial direction as the temperature decreases or the diameter of particles in the reactor decreases.

.

CONCLUSIONS: In this work, it was revealed that the visualization of flow behaviors of heavy oils in the packed-bed reactor at high temperature and high pressure is feasible by neutron radiography.

REFERENCES:

[1] K. Sugioka *et al.*, *AIChE J.*, **60**, (2014) 1168.

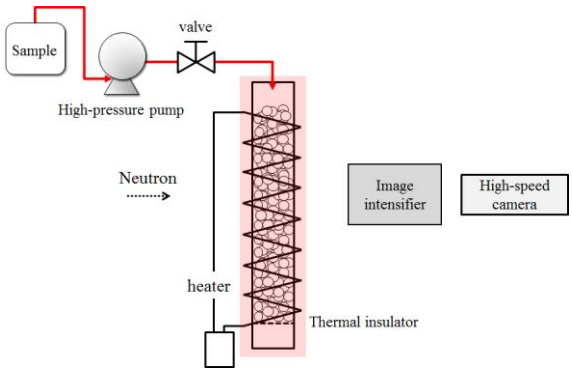

Figure 1 Schematic diagram of the apparatus

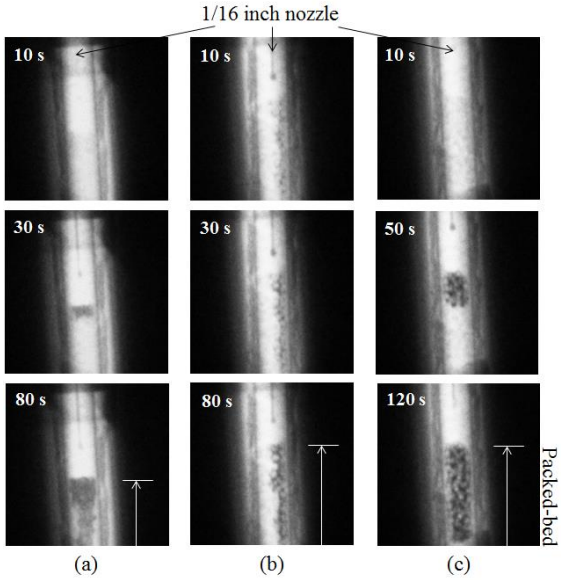

Figure 2 Neutron radiographs of flow behaviors of bitumen through the packed-bed.

PR2-4 Estimation of the Frosting and Defrosting Phenomena by Using Netron Radiography

R. Matsumoto, K. Kagebayashi[1], T. Uechi[1], D. Ito[2] and Y. Saito[2]

Faculty of Engineering Science, Kansai University
[1]Graduate School of Science and Engineering, Kansai University
[2]Research Reactor Institute, Kyoto University

INTRODUCTION:

Heat exchangers which are operated at below 0 °C are subjected to the frost deposition and its growth. Frost formation on heat exchangers has a serious impact on the heat transfer performance in two ways; one is a thermal resistance between the cold surface and the humid ambient air, the other is an air-side pressure drop by the blockage effect of the frost layer. In spite of the relatively large number of articles, there are still gaps between the analytical model and the experimental results. One of the reasons is the difficulty to evaluate the mass transfer coefficient for the frost deposition.

On the cooled surface of a heat exchanger, the frost grows with a spatial distribution that is determined by the temperature and humidity profiles of the air and the flow pattern in the heat exchanger. This means that the mass transfer coefficient for frost formation has both temporal and spatial distribution. However, in conventional methods of measuring the frost accumulation rate, the frost is scraped from the surface, or the frost accumulation is estimated from the difference between the absolute humidities before and after the heat exchanger. In the present study, the frost formation and defrosting process was estimated by the two ways by neutron and X-ray radiographies at KUR B-4 radiation port.

ESTIMATION DEFROSTING PROCESS BY NEUTRON RADIOGRAPHY:

The frost layer with defrosting process was measured by using a neutron radiography in the defrosting process on the aluminum finned-tube heat exchanger under the forced-convection. The heat exchanger is shown in Fig.1. Fins have dimensions of 60mm in height, 28mm in width and 0.12mm in thickness.

The water deposition distributions were estimated quantitatively in every 5 seconds for 10 minutes of the defrosting period. The melting water behavior was investigated by comparing the water deposition distribution before defrosting. The initial stage of the defrosting was referred to as the melting progressing period, in which the melting water penetrated into the water permeation layer in the frost thickness direction, as shown in t=140sec. of Fig.2. After 180sec from starting the defrosting process, the frost at the fin front edge and the surrounding the tubes were melted, then, the water permeation layer was saturated by the melting water. The neutron radiography images, as shown at t=380 sec. of Fig.2, indicated the melting water penetration into the spanwise direction of the fins. The total migration volume of the melting water into the spanwise direction was about 30% of the total frost deposition.

MEASUREMENT OF FROST DENSITY PROFILE BY X-RAY RADIOGRAPHY:

Frost is the porous material of the crystal ice and air. The low thermal conductivity of the frost causes the low heat transfer performance. The frost density profile of the frost layer is the important property for the frost formation estimation. The frost formation process was measured by the X-ray radiography (XRG) on the cylindrical cooling surface.

The frost density profiles is shown in Fig. 3 at the 22.5mm from the reading edge of the cylindrical cooling surface. The experimental results clearly shows the development of the frost layer density.

CONCLUSIONS:

The neutron and X-ray radiographies are effectiveness for the frost layer measurement.

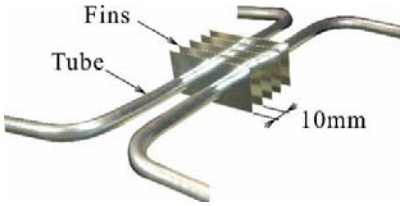

Fig.1 Plate-fin tube heat exchanger.

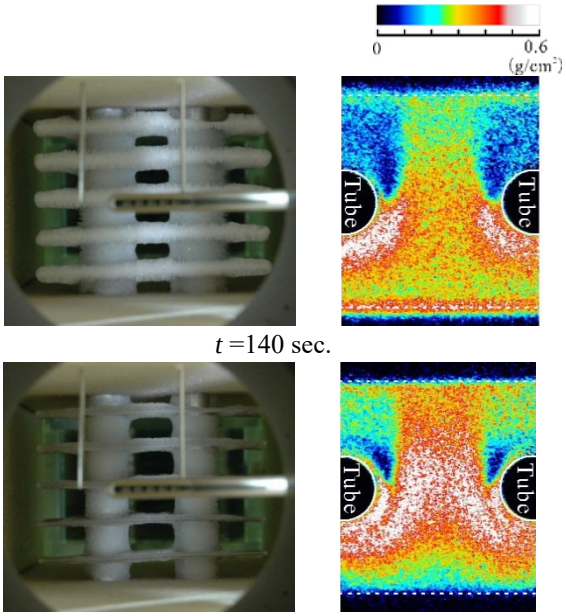

t =140 sec.

t =380 sec.

(a) Digital camera image (b) Water deposition m_w

Fig.2 Water deposition profiles on the fins.

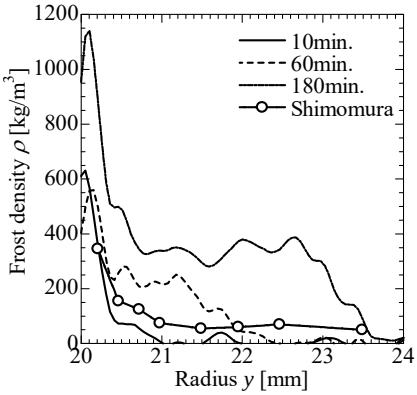

Fig.3 Distribution of frost density with height.

27P2-6